J Mater Sci: Mater Electron (2010) 21:1030–1035
DOI 10.1007/s10854-010-0084-0

Effects of Al content on the properties of ZnO:Al films prepared by Al_2O_3 and ZnO co-sputtering

Zhonghua Deng · Changgang Huang · Jiquan Huang · Meili Wang · Hong He · Hai Wang · Yongge Cao

Received: 18 December 2009 / Accepted: 15 February 2010 / Published online: 27 February 2010

Abstract Aluminum doped zinc oxide (AZO) films were deposited on quartz substrates by radio-frequency magnetron co-sputtering method with ZnO and Al_2O_3 ceramic targets. The structural, optical and electrical properties of these films as a function of the Al content were investigated. XRD results reveal that the AZO films are wurtzite structure with (002) preferred orientation. The average transmittance of all the films is higher than 80% in a wide wavelength range from 400 to 1,500 nm. The band gap energy, calculated from their optical absorption spectra, is in the range of 3.50–3.66 eV depending on the Al content. Doping of Al^{3+} in the ZnO makes the film surface roughness decrease. The dopant Al^{3+} acts as electron donor by which the electrical conductivity and carrier concentration of the films are obviously increased until the Al^{3+} reaches its saturation content of about 4.50 at.%.

1 Introduction

ZnO semiconductor with a direct band gap of 3.3 eV, which has been intensively investigated, has a high transmittance in the visible range. In addition, doping of the IIIA ions into the lattice reduces its resistivity without any deterioration of its transmittance [1, 2]. Thus, it follows into the transparent conducting oxides (TCO) family which has wide application in liquid crystal and flat panel display, solar cells, and organic light-emitting devices [3–6]. Comparing to other TCOs, such as the indium tin oxide (ITO), indium zinc oxide (IZO) and fluorine tin oxide (FTO), the alumina zinc oxide (AZO) holds advantages in the aspects of low cost, free of toxics and stability against hydrogen plasma [7, 8]. Due to these, the AZO film has been considered to be the most potential alternative to ITO, which has already been extensively adopted as transparent conducting films material but is becoming extremely expensive because of running short of the rare metal indium. Therefore, investigation of the preparation and properties of the AZO films is highly demanded.

Growth of the AZO films has so far been carried out by sputtering deposition [7–9], pulsed laser deposition (PLD) [10], evaporation [11], metal–organic chemical vapor deposition (MOCVD) [12], spray paralysis [13] and sol–gel method [14]. Among them, the sputtering is one of the most widely used techniques because of its advantages such as high deposition rate, good adhesion of film on substrate and low deposition temperature [15]. Two types of sputtering strategies are commonly applicable according to the Al doping method. One is the conventional sputtering of a ZnO/Al_2O_3 composite target [16] or reactive sputtering from a metallic Zn/Al alloy target [17], the other is co-sputtering [18–20]. Between them, it is more freely for the co-sputtering process to control the concentration of the doping element Al which is of the determining aspect on the properties of the AZO films. So far, most co-sputtering methods are concentrated on the reactive sputtering with an Al metal target and a ZnO ceramic target or two

Z. Deng · C. Huang · J. Huang · M. Wang · H. He · H. Wang · Y. Cao (✉)
Key Laboratory of Optoelectronic Materials Chemistry and Physics, Fujian Institute of Research on the Structure of Matter, Chinese Academy of Sciences, 350002 Fuzhou, Fujian, People's Republic of China
e-mail: caoyongge@fjirsm.ac.cn

Z. Deng
e-mail: dengzhonghua@fjirsm.ac.cn

Z. Deng · M. Wang
Graduate University of Chinese Academy of Sciences, 350002 Fuzhou, Fujian, People's Republic of China

metallic targets. Little reports have been presented in the literature about the co-sputtering method with Al_2O_3 and ZnO ceramic targets.

In this paper, we presented a detailed investigation of the preparation and properties of the AZO films by co-sputtering method with Al_2O_3 and ZnO ceramic targets. Discussions are carried out to elucidate the effects of the Al content on the structural, optical and electrical properties of the films.

2 Experimental details

All AZO films were deposited on quartz glass substrates by a RF magnetron sputtering system. This system can accommodate four water-cooled 2 inches targets with a thickness of 3 mm. However, it makes the substrate inclined by about 30° with respect to the sputtering targets. The distance between the center of the targets and the substrate was about 11 cm. The substrate holder was rotated at 8 rotations per minute about its axis. Two target holders in opposite position were selected. Deposition was carried out by co-sputtering method with a self-made Al_2O_3 ceramic target and a commercial ZnO target (99.99%). High purity Ar gas (99.999%) was used as the working gas and introduced into the chamber by a mass flow controller with flow rate fixed at 20 sccm (standard cubic centimeter per minute). Before deposition, the sputtering chamber was evacuated by a turbo molecular pump to a background pressure of 2×10^{-4} Pa and the targets were pre-sputtered for 10 min in order to remove possible contamination on the surface. Quartz glass was used as the substrate after cleaning by ultrasonic bath in acetone, alcohol and de-ionized water for 10 min sequentially. After transferring into the chamber, it was further cleaned by anti-sputtering for 3 min. The substrate placed upon the targets was heated and rotated. The substrate temperature was set to be 400 °C. The working pressure was fixed at 0.15 Pa. The alumina content in the AZO films was controlled by changing the RF power of the Al_2O_3 target from 50 to 100 W and fixing the RF power of ZnO target at 100w. The deposition was carried out for 30 min.

The phase and crystal structure of the deposited AZO films were determined by X-ray diffraction (XRD, DMAX2500, RIGAKU, Japan). The film thickness and surface morphology was examined by field emission scanning electron microscopy (FE-SEM, JSM6700F, JEOL, Japan) and atomic force microscope (AFM, Nanoscope NS3A-02, Veeco, USA). The chemical composition was determined by energy dispersive spectroscopy (EDS) attached to the FE-SEM. The optical transmittance of the films was measured by a UV–Vis spectrophotometer (Lambda 900, Perkin Elmer, USA). The electrical properties were examined by a HL55WIN Hall System using van der Pauw geometry.

3 Results and discussion

3.1 Film structure

The Al content of the doped ZnO films was approximately estimated by the (EDS). Only signals from the O, Si, Al and Zn atoms were detected in EDS measurements. The Al content results (the atomic ratio of Al to Al + Zn) of the AZO films with different Al_2O_3 target RF power were calculated from the EDS are depicted in Fig. 1. As shown in Fig. 1, the Al content increases almost linearly with Al_2O_3 target RF power. Correspondingly, doping concentration of Al^{3+} varies from 1.80 to 8.06 at.% in the ZnO films was obtained.

The crystal structure of the AZO films was determined by XRD. As presented in Fig. 2, only the (002) diffraction peak of the wurtzite ZnO structure is observed, which indicates the AZO films grow along <0001> direction. The preferred orientation growth of ZnO films with *c*-axis perpendicular to the substrate surface was attributed to self-texturing [21]. No diffraction peaks from the possible secondary phases, such as Zn, Al, Al_2O_3 and the ternary phase of $ZnAl_2O_4$, were detected, suggesting that aluminum may substitutionally replace zinc in the hexagonal lattice, interstitially exist in the ZnO lattice or segregate into the non-crystalline region in grain boundaries [8]. The (002) peak of zinc oxide film occurs at 34.01°. With the increase of Al content, this peak shifts to higher 2θ values initially, and then reaches the maximum value of 34.27° at

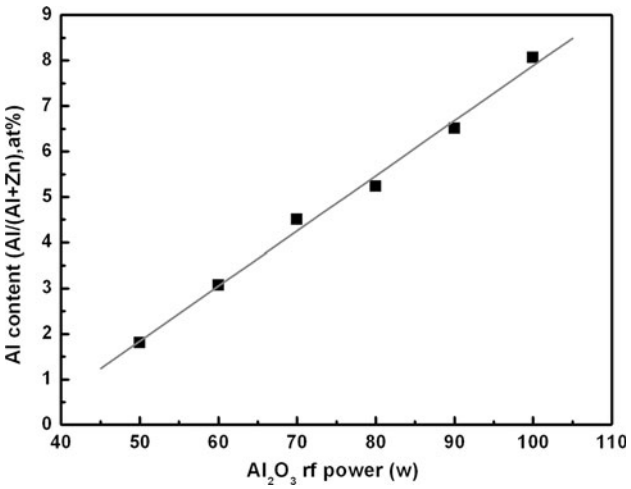

Fig. 1 Al content of the AZO films with various Al_2O_3 target RF power determined from EDS

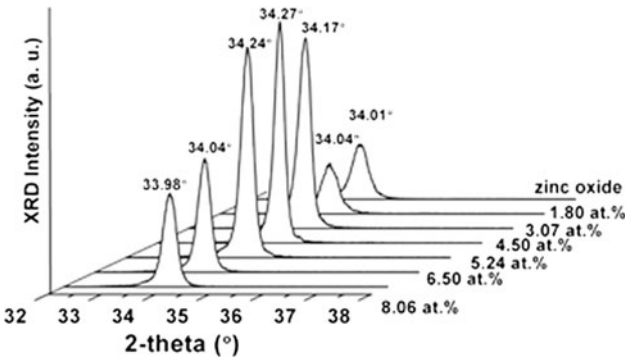

Fig. 2 XRD patterns of AZO films

AZO film with 4.50 at.% of Al, after that the peak position shifts to lower 2θ values. When Al ions substitute the Zn ions in ZnO, the lattice parameters decrease because the ionic radii of Al^{3+} (0.54 nm) is smaller than that of the Zn^{2+} (0.74 nm). This may be the reason that the (002) peaks shift to higher 2θ values. However, if the segregations of Al atoms happen when Al is over a certain content, the (002) peaks may shift back to lower 2θ value.

Figure 3 shows the FE-SEM images of zinc oxide and AZO films with Al content of 1.80 at.%. The FE-SEM images show that the morphology of the grains of zinc oxide film (undoped) is quite different from that of the Al^{3+} doped ones. The zinc oxide film presents a pyramidal shape with a crystal size of 120–180 nm. However, the AZO film with Al content of 1.8 at.% presents a fusiform shape with a much smaller crystal size. Similar phenomenon was observed in AZO films deposited by co-sputtering from sintered ZnO and Al targets [22]. The insets in Fig. 3 show the corresponding cross-section of the zinc oxide and AZO films. Both of them show a compact columnar structure. The film thicknesses can be obtained from the cross-section images. The film thicknesses of undoped zinc oxide films were 200 ± 20 nm. The thicknesses of doped zinc oxide films were all 300 ± 20 nm regardless of Al_2O_3 target RF power. The thickness values of deposited AZO films were confirmed by step test of AFM which are in consistence with the SEM results. These results indicate that co-sputtering with Al_2O_3 not only influences surface morphology but also increases the growth rate of the film.

Figure 4 shows the AFM images of ZnO and AZO films with different Al content. The measured root-mean-square (RMS) roughness values are also listed in each image, respectively. It is shown that the crystal grain size and roughness values decrease with increasing Al_2O_3 content in the films, which may be attributed to the low surface diffusion length of Al. As the Zn and Al adatoms impinge on the substrate, Al may prevent the migration and incorporation of the Zn adatoms.

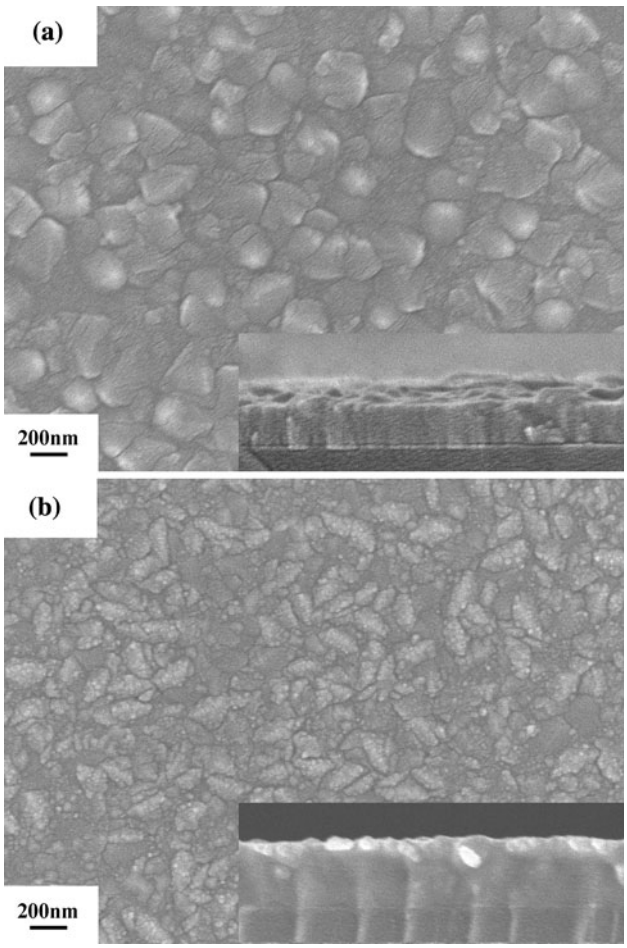

Fig. 3 Surface morphology and cross-section of **a** zinc oxide film and **b** AZO film with Al content of 1.80 at.%

3.1.1 Optical properties

The transmittance of the deposited films with different Al content was measured at room temperature and the resulting transmittance spectra was shown in Fig. 5. It may be seen that all the films are highly transparent over the visible and near infrared regions from 400 to 1,500 nm. The average transmittance of the films were calculated and listed in Table 1. The average transmittance of all the films is over 80% in quite a wide wavelength range, which is close to that of the conventional ITO films, indicating that these materials are suitable for transparent electrode. The optical transmittance of the doped ZnO is enhanced by incorporation of moderate content of aluminum. The average transmittance decreases as further increases of the Al content, which may be due to the segregation of Al atoms into the non-crystalline grain boundary. As clearly shown from the inset of Fig. 5, the UV absorption edges shift to shorter wavelength (blue shift) when Al is incorporated, and then to a longer wavelength (red shift) when Al content is over 4.50%. Optical band gap (E_g) of the

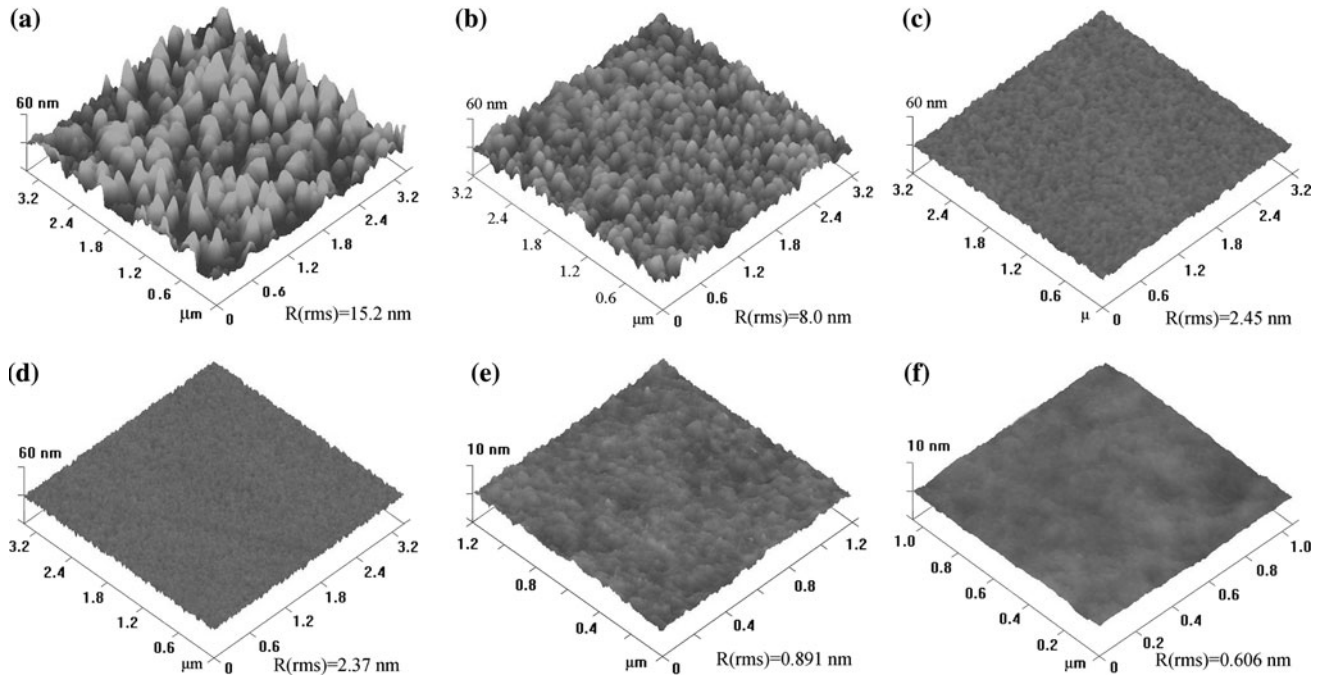

Fig. 4 AFM images of **a** ZnO and AZO films with different Al content **b** 1.80 at.%, **c** 3.07 at.%, **d** 4.50 at.%, **e** 5.24 at.% and **f** 6.51 at.%

films was estimated by the optical absorption method. The absorption coefficient was calculated from the optical spectra of the films by using the equation $\alpha = 1/d \times \ln[(1 - R)/T]$ with the knowledge of film thickness d, reflectance R and transmittance T [23]. On the other hand, the squared absorption coefficient of a semiconductor with a direct band structure can also be expressed as $(\alpha_{hv})^2 = C\ (hv - E_g)/hv$, where hv, E_g are the photo energy and band gap energy, respectively, and C is a related constant. By extrapolating the linear part of the curve in the $(\alpha_{hv})^2$ versus hv plot to the energy axis, the value of band gap energy can thus be determined at the interception point [16]. Figure 6 shows the relationship between α^2 and hv. From Fig. 6, E_g of undoped ZnO is 3.26 eV which is close to the theoretical band gap energy of the ZnO (3.3 eV), and the E_g values for the AZO films with various Al content are listed in Table 1. As the increase of Al^{3+} doping concentration, the energy band gap of AZO film initially increases and reaches the maximum value of 3.66 eV at Al content of 4.50 at.%, then decreases when Al content further increases. Both the widening and narrowing of the band gap are observed in the present case with Al^{3+} content increasing. The reasons may be as follows. The band gap widening is associated with the lowest states of the blocked conduction band, which is the well-known Burstein–Moss effect [24], while the narrowing originates from the different many-body effects such as energy exchange due to electron–electron and electron–impurity interactions on the conduction and valence bands [25].

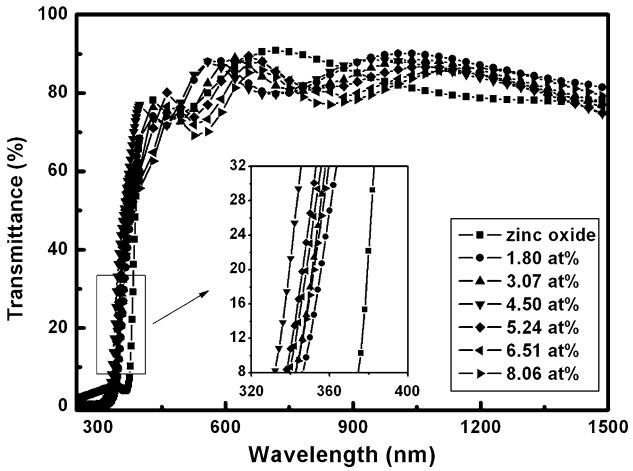

Fig. 5 The transmittance spectra of the AZO films with Al content varying from 0 to 8%

3.1.2 *Electrical properties*

ZnO always has a small oxygen deficiency under ordinary circumstance which results in a typical resistivity of 1–100 Ω cm [24]. Al acts as a cationic dopant in the ZnO lattice and substituted the Zn site. In ZnO, since zinc has a valence of 2, the aluminum doping in the lattice provides electrons to the conduction band and drastically reduce the resistivity of ZnO [26]. Figure 7 shows the electrical properties of the AZO films with various Al content. The resistivity ρ, hall mobility μ and carrier concentration n of undoped ZnO were 0.34 Ω cm, 5.5 $cm^2V^{-1}\ s^{-1}$ and $3.3 \times 10^{18}\ cm^{-3}$,

Table 1 The average transmittance in the wavelength range from 400 to 1,500 nm and the calculated optical band gap of the AZO films with various Al content

Al content (at.%)	0	1.80	3.07	4.50	5.24	6.51	8.06
Average transmittance (%, 400–1,500 nm)	81.85	84.35	83.06	82.51	82.07	80.94	80.37
Optical band gap (eV)	3.26	3.50	3.56	3.66	3.62	3.60	3.56

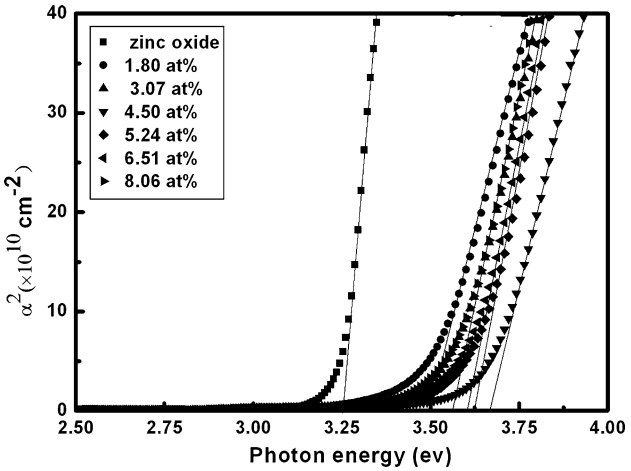

Fig. 6 The optical band gap of the as-deposited films with Al content varying from 0 to 8 at.% calculated from their transmittance spectra

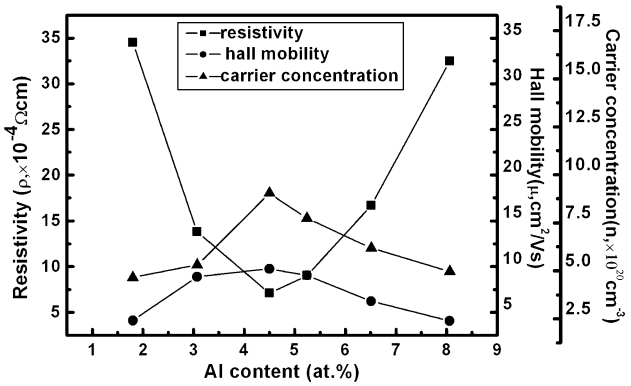

Fig. 7 Electrical properties of AZO films with various Al content

respectively. Ordinarily, the conduction of undoped ZnO was attributed to O^{2-} vacancy and Zn interstitials [27]. The high carrier concentration of 3.3×10^{18} cm^{-3} indicates that a large amount of intrinsic defects exist in the undoped ZnO film which may result in lower crystallinity, transmittance and hall mobility. The resistivity of ZnO film dramatically decreases with Al^{3+} doping due to Al^{3+} substitution of Zn^{2+}, oxygen vacancies and Zn interstitial atoms [28]. As Al content increases, the resistivity of AZO films decreases initially and reaches a minimum of 7.1×10^{-4} Ω cm at a Al content of 4.50 at.%, then increases to 3.2×10^{-3} Ω cm at a Al content of 8.06 at.%. The resistivity is inversely proportional to the product of the Hall mobility μ and the carrier concentration n, that is the relation $\rho = 1/(e\ \mu\ n)$, where e is electron charge. The minimum resistivity is achieved when both Hall mobility and carrier concentration are at a high lever. Both carrier concentration and Hall mobility increase with Al content and reach a maximum value at 4.50 at.%, and then decrease as Al content further increases. The carrier concentration of AZO films at a Al content of 8.06 at.% is much lower than that of the film with 4.50 at.% Al^{3+}, which suggests that excess Al atoms may not be active due to segregation to the non-crystalline grain boundary [16]. The mobility reaches a maximum with moderate donors may be attributed to the improvement of film crystalline [7, 27], which is in good agreement with the XRD measurement listed in Fig. 2.

4 Conclusions

AZO films were prepared on quartz glass substrates by RF magnetron co-sputtering method with ZnO and Al_2O_3 ceramic targets. A thorough investigation, summarized by the crystal structure determination, film morphology observation, transmittance spectra measurement, optical band gap calculation and electrical properties evaluation, were carried out to make an examination of the effects of the Al^{3+} content on the properties of the AZO films. The EDS results show that the Al^{3+} content increases almost linearly with increasing of the RF power of the Al_2O_3 target. The XRD results reveal the deposited AZO films is of single phase and wurtzite structure with highly preferred (002) orientation. The FE-SEM micrographs show that the morphology of the crystal grain for zinc oxide film (undoped) is quite different from that of the AZO film with Al content of 1.80 at.% (doped). The AFM images show that the film roughness decreases with the Al^{3+} content in the films, which may be due to the low surface diffusion length of Al. The transmittance measured over the visible and near-infrared spectra range is higher than 80% which is close to the commercial ITO films. The dopant Al^{3+} in the ZnO lattice may substitute the Zn^{2+} site and act as electron donor which makes the electrical conductivity and carrier concentration increase. As the Al^{3+} content increase to 4.50 at.%, these values reach the maxima and then decrease with Al^{3+} content further increase.

Acknowledgments This work is finally supported by the National Basic Research Program (grant no 2007CB936700), Key Program of

Sci. & Tech. in Fujian Province(no 2009I0028), the National Natural Science Foundation of China (20901079).

References

1. U. Ozgur, Y.I. Alivov, C. Liu, A. Teke, M.A. Reshchikov, S. Dogan, V. Avrutin, S.J. Cho, H. Morkoc, J. Appl. Phys. **98**, 041301 (2005)
2. Y. Imai, A. Watanabe, J. Mater. Sci. Mater. Electron. **15**, 743 (2004)
3. C.G. Granqvist, Appl. Phys. A Mater. Sci. Process. **57**, 19 (1993)
4. T. Minami, Semicond. Sci. Technol. **20**, S35 (2005)
5. G.J. Exarhos, X.D. Zhou, Thin Solid Films **515**, 7025 (2007)
6. T.W. Kim, D.C. Choo, Y.S. No, W.K. Choi, E.H. Choi, Appl. Surf. Sci. **253**, 1917 (2006)
7. C. Jeong, H.S. Kim, D.R. Chang, K. Kamisako, Jpn. J. Appl. Phys. **47**, 5656 (2008)
8. J. Hong, H. Paik, H. Hwang, S. Lee, A.J. Demello, K. No, Phys. Status Solidi. A Appl. Mater. **206**, 697 (2009)
9. S.N. Bai, T.Y. Tseng, J. Mater. Sci. Mater. Electron. **20**, 253 (2009)
10. Z.Y. Ning, S.H. Cheng, S.B. Ge, Y. Chao, Z.Q. Gang, Y.X. Zhang, Z.G. Liu, Thin Solid Films **307**, 50 (1997)
11. J. Ma, F. Ji, D.H. Zhang, H.L. Ma, S.Y. Li, Thin Solid Films **357**, 98 (1999)
12. S.Y. Myong, S.J. Baik, C.H. Lee, W.Y. Cho, K.S. Lim, Jpn. J. Appl. Phys. **36**, L1078 (1997)
13. B.-O.P. Jin-Hong Lee, Mater. Sci. Eng. B **106**, 242 (2004)
14. S. Mridha, D. Basak, J. Phys. D Appl. Phys. **40**, 6902 (2007)
15. K. Ellmer, J. Phys. D Appl. Phys. **33**, R17 (2000)
16. K.H. Kim, K.C. Park, D.Y. Ma, J. Appl. Phys. **81**, 7764 (1997)
17. C. Major, A. Nemeth, G. Radnoczi, Z. Czigany, M. Fried, Z. Labadi, I. Barsony, Appl. Surf. Sci. **255**, 8907 (2009)
18. K. Tominaga, M. Kataoka, H. Manabe, T. Ueda, I. Mori, Thin Solid Films **291**, 84 (1996)
19. B.Y. Oh, M.C. Jeong, W. Lee, J.M. Myoung, J. Cryst. Growth **274**, 453 (2005)
20. Y.M. Chung, C.S. Moon, M.J. Jung, J.G. Han, Surf. Coat. Technol. **200**, 936 (2005)
21. X. Jiang, C.L. Jia, B. Szyszka, Appl. Phys. Lett. **80**, 3090 (2002)
22. S. Mandal, H. Mullick, S. Majumdar, A. Dhar, S.K. Ray, J. Phys. D Appl. Phys. **41**, 6 (2008)
23. S.B. Qadri, H. Kim, J.S. Horwitz, D.B. Chrisey, J. Appl. Phys. **88**, 6564 (2000)
24. E. Burstein, Phys. Rev. **93**, 632 (1954)
25. B.E. Sernelius, K.F. Berggren, Z.C. Jin, I. Hamberg, C.G. Granqvist, Phys. Rev. B **37**, 10244 (1988)
26. R.B.H. Tahar, T. Ban, Y. Ohya, Y. Takahashi, J. Appl. Phys. **83**, 2631 (1998)
27. K. Tominaga, H. Manabe, N. Umezu, I. Mori, T. Ushiro, I. Nakabayashi, J. Vac. Sci. Technol. A **15**, 1074 (1997)
28. S.S. Lin, J.L. Huang, P. Sajgalik, Surf. Coat. Technol. **190**, 39 (2005)